Proceedings of IMECE04
2004 ASME International Mechanical Engineering Congress and Exposition
November 13-20, 2004, Anaheim, California USA

IMECE2004-61665

THERMAL CONDUCTIVITY OF SINGLE-WALL CARBON NANOTUBES

Hongliang Zhong **Jennifer R. Lukes**

Department of Mechanical Engineering and Applied Mechanics
University of Pennsylvania
Philadelphia, PA, 19104-6315

ABSTRACT

Despite the significant amount of research on single-wall carbon nanotubes, their thermal conductivity has not been well established. To date only one experimental thermal conductivity measurement has been reported for these molecules around room temperature, with large uncertainty in the thermal conductivity values. Existing theoretical predictions based on molecular dynamics simulation range from several hundred to 6600 W/m-K. In an attempt to clarify the order-of magnitude discrepancy in the literature, this paper utilizes molecular dynamics simulation to systematically examine the thermal conductivity of several (10, 10) single-wall carbon nanotubes as a function of length, temperature, boundary conditions and molecular dynamics simulation methodology. The present results indicate that thermal conductivity ranges from about 30 – 300 W/m-K depending on the various simulation conditions. The results are unconverged and keep increasing at the longest tube length, 40 nm. Agreement with the majority of literature data is achieved for the tube lengths treated here. Discrepancies in thermal conductivity magnitude with experimental data are primarily attributed to length effects, although simulation methodology, stress, and intermolecular potential may also play a role. Quantum correction of the calculated results reveals thermal conductivity temperature dependence in qualitative agreement with experimental data.

Keywords: thermal conductivity, molecular dynamics simulation, phonon, single-wall carbon nanotube

NOMENCLATURE

$\overline{B}_{ij}$	= bond order term in BOP
BOP	= bond order potential
c	= speed of sound
$D(\omega)$	= density of states
ε	= atomic energy including both potential and kinetic
EMD	= equilibrium molecular dynamics
E_{pot}	= total bonded potential energy
$\overrightarrow{f_{ij}}$	= force on atom i due to atom j
$\overrightarrow{F_e}$	= external force field in homogeneous NEMD
$\overrightarrow{F_i}$	= total force on atom i
HCACF	= heat current autocorrelation function
$\hbar$	= Planck constant / 2π
J	= heat current
k	= thermal conductivity
k_B	= Boltzmann constant
L	= tube length
m	= atomic mass
MD	= molecular dynamics
MWNT	= multi-wall carbon nanotube
N	= number of atoms
N_{cell}	= number of unit cells
NEMD	= nonequilibrium molecular dynamics
PBC	= periodic boundary conditions
r_{ij}	= distance between atom i and j
$\vec{r}$	= atomic position vector
SWNT	= single-wall carbon nanotube
t_{corr}	= correlation time
t_{run}	= simulation run time
τ_1, τ_2	= time constant in double exponential fit for HCACF
T	= temperature
T_{MD}	= MD temperature
$U_B(r_{ij})$	= bonded potential energy between atom i and j
υ	= frequency
$\vec{v}$	= atomic velocity vector
V	= volume
$V_A(r_{ij})$	= attractive pair term in BOP
$V_R(r_{ij})$	= repulsive pair term in BOP
ω	= angular frequency
$\vec{\omega}$	= angular velocity of simulation system

ω_D = Debye frequency

x = Cartesian coordinate

σ_k = probable error of thermal conductivity

σ_T = probable error of temperature

$\sigma_{<J(t)J(0)>}$ = probable error of HCACF

$< >$ = ensemble average

SUBSCRIPTS

α , β = directional index

i, j, k = summation index, atom index

INTRODUCTION

Recent advances in shrinking the size of micro and nano devices have made thermal management critically important to continued high performance, reliability and lifetime. Materials that have high thermal conductivity and therefore help transfer heat efficiently are of great interest in those applications where operating temperatures have a significant impact on devices. Carbon nanotubes (CNTs) show thermal properties that are remarkably different from other known materials and are expected to be a promising candidate in many applications. Most measurements of k (T) on nanotube materials show that k increases monotonically with increasing T even above ambient temperature. Kim et al. [1] observed that the thermal conductivity of an individual MWNT with a diameter of 14nm is more than 3000 W/m-K at room temperature. Hone et al. [2] found that the thermal conductivity of aligned single-wall nanotube (SWNT) crystalline ropes is about 250 W/m-K at 300K and estimated that the longitudinal thermal conductivity of a single SWNT ranges from 1750 to 5800 W/m-K. Tubes can be microns long and the predominant diameter of each individual tube is 1.4nm. A recent measurement on an isolated SWNT reveals a higher thermal conductivity than that of MWNT [3], but there is large uncertainty in the measured values.

Molecular dynamics simulation (MD) [4] is an alternative method to determine the thermal conductivity of carbon nanotubes, and yields additional atomistic information useful for analyzing thermal energy transport in SWNT and in carbon nanotube based materials. Classical MD involves integration of Newton's equations of motion for atoms interacting with each other through an empirical interatomic potential that does not include modeling electrons and therefore cannot simulate electron-electron or electron-phonon interactions. Measurements indicate that phonon contribution for thermal conductivity is dominant in both MWNTs and SWNTs at all temperatures [5], which justifies neglecting electronic effects in simulations of carbon nanotubes.

In general there are three ways to compute the thermal conductivity in a solid. Nonequilibrium molecular dynamics (NEMD) [6] is based on Fourier's law which relates the heat current to the temperature gradient through thermal conductivity

$$J_\alpha = -\sum_\beta k_{\alpha\beta} \partial T / \partial x_\beta \tag{1}$$

NEMD, also called the direct method, imposes either a fixed temperature gradient or a heat flux to a system. In order for fast convergence of the resultant heat flux or temperature field and also because of the nanoscale size of SWNT, NEMD involves large temperature gradients beyond the range that can be reached experimentally. A disadvantage of NEMD is that in order to obtain the thermal conductivity along multiple coordinate directions in a solid, a separate simulation must be run in each direction. In contrast, a thermal conductivity tensor can be obtained in just one simulation by equilibrium molecular dynamics (EMD) [7]. The EMD method is based on the Green-Kubo formula derived from linear response theory [8]

$$k_{\alpha\beta} = \frac{1}{Vk_BT^2}\int_0^\infty < J_\alpha(t) \bullet J_\beta(0) > dt \tag{2}$$

where the heat current is written as [9]

$$\vec{J} = \frac{d}{dt}\sum_i \vec{r_i}(t)\varepsilon_i(t) \tag{3}$$

and the term inside the brackets represents the heat current autocorrelation function (HCACF). The temporal decay of the HCACF represents the time scale of thermal transport.

The atomic energy that each individual atom has is taken to be

$$\varepsilon_i = \frac{1}{2}m_i\vec{v}_i \bullet \vec{v}_i + \frac{1}{2}\sum_j u_B(r_{ij}) \tag{4}$$

The third method, homogeneous NEMD[10], is an nonequilibrium approach in which an external field is applied to the system to represent the effects of heat flow without physically imposing a temperature gradient or flux. $\overrightarrow{F_e}$ is the external field that adds an extra force to each individual atom by

$$\Delta\overrightarrow{F_i} = (\varepsilon_i - < \varepsilon >)\overrightarrow{F_e} - \sum_{j(\neq i)} \overrightarrow{f_{ij}}(\overrightarrow{r_{ij}} \bullet \overrightarrow{F_e}) + \frac{1}{N}\sum_{jk(j\neq k)} \overrightarrow{f_{jk}}(\overrightarrow{r_{jk}} \bullet \overrightarrow{F_e}) \tag{5}$$

Extrapolation to zero force [10] allows the thermal conductivity to be determined from

$$k_\alpha = \lim_{\overrightarrow{F_e}\to 0}\lim_{t\to\infty}\frac{< J_\alpha(\overrightarrow{F_e}, t) >}{F_eTV} \tag{6}$$

where the heat current $J_\alpha(\overrightarrow{F_e}, t)$ is also evaluated as in Eq. 3. This method is computationally efficient, but the extrapolation to zero $\overrightarrow{F_e}$ can be a challenge as is shown later.

Several classical MD simulations have been performed in order to pinpoint the thermal conductivity of isolated SWNT [11-16]. These results, which vary from several hundred to 6600 W/m-K, show an order of magnitude discrepancy. The range of this spread is comparable to that observed in the experimental measurement [3], but in general the simulated values are lower. As the structural details of the tube measured in the experiment are not known, it is difficult to compare to simulations on specific tube chiralities. There is still significant uncertainty as to the correct value of SWNT thermal conductivity.

Berber et al. [11] used homogeneous NEMD for an isolated (10, 10) SWNT with periodic boundary conditions (PBC). Cross sectional area, which affects thermal conductivity through the volume V in Eq. (2), was calculated based upon the fact that tubes have an interwall separation about 3.4Å in nanotube bundles. The thermal conductivity increases with increasing temperature, then reaches a peak at around 100K, finally decreasing to about 6600 W/m-K at room temperature. Osman et al. [12] also found a peaking behavior of thermal conductivity before falling off around 400K for (10, 10) SWNTs. NEMD and PBC were used. The thermal conductivity is about 1700W/m-K at 300K. A ring of van der Waals thickness 3.4Å was used in the calculations as the cross sectional area for heat flow. Che et al. [13] applied EMD based on the Green-Kubo theory with PBC and claimed to find length convergent behavior of thermal conductivity for (10, 10) SWNT about 2980 W/m-K at room temperature. The maximum length tube was around 40 nm (6400 atoms) and a ring of 1Å thickness for the cross sectional area was chosen as the geometric configuration. Padgett et al. [14] used NEMD with PBC and predicted thermal conductivity about 160 W/m-K for 61.5 nm long (10, 10) SWNT at 300K. Moreland et al. [15] used NEMD with PBC and found that the thermal conductivity of (10, 10) SWNT at 300K increases from 215W/m-K at 50 nm to 831 W/m-K at 1000 nm tube length. The cross sectional area was calculated as the area of a circle with circumference defined by the centers of the atoms around the nanotube, which is different from [13]. Only Maruyama [16] did not use PBC to simulate finite-length SWNTs. The cross sectional area was defined in the same way as that in [12]. The thermal conductivity is around 600W/m-K for a 404nm long tube and still steadily increasing with an exponent of 0.27. The latter two results indicate that length convergence is still not achieved even for the longest tubes simulated.

Table 1 lists the room temperature thermal conductivity results found in the above studies. Part of the difference between the results of the various groups can be attributed to differing choices for nanotube cross sectional area, but scaling all tubes by the same area still does not eliminate the differences. All of the simulations described above, except [14], use the Tersoff-Brenner bond order potential (BOP) [17] to model the carbon nanotubes. Padgett et al [14] use the reactive bond order potential [18]. Differences in simulation methodology, boundary conditions, tube length, and potential may contribute to the observed differences.

Table 1 Thermal Conductivity Values from Different Groups

	k (W/m-K)	tube length (nm)	cross sectional area (m^2)
Berber et al. [11]	6600	2.5	29×10^{-19}
Osman et al. [12]	1700	30	14.6×10^{-19}
Che et al. [13]	2980	40	4.3×10^{-19}
Padgett et al. [14]	160	61.5	14.6×10^{-19}
Moreland et al. [15]	215	50	14.6×10^{-19}
Maruyama [16]	310	40	14.6×10^{-19}
Experimental measurement			
Kim et al. [1]	3000 W/m-K for MWNT		
Yu et al. [3]	more than 3000 W/m-K for SWNT		
All values are at 300K			

Moreland et al. [15] determined the stress-free tube length by running simulations with free boundaries at the tube ends to allow for longitudinal expansion/contraction, and then applied PBC for the remainder of the simulations. They found much lower thermal conductivity than that from experiments and from some simulations of other researchers above. As no mention of efforts to mitigate stress by relaxing the structure is discussed in these papers, it is possible that some of the high calculated values [11-13] may be caused by compression of the tubes, but this is not certain. Stress/strain effects have already been demonstrated to be important in other nanostructures [19]. The stress state of the experimental measurements is unknown.

It is not clear whether EMD or NEMD is better for simulating SWNT [15]. The effect of artificially imposing a highly nonlinear temperature gradient or heat flux in NEMD compared to EMD remains to be seen, if both techniques use the same BOP code and apply to the same SWNT. Another important difference between EMD and NEMD comes from the axial boundary condition. The phonon mean free path in SWNT is several microns [20]. Therefore thermal conductivity is believed to be length dependent not only because longer tubes can sustain more phonon modes but because the tube boundaries introduce another phonon scattering mechanism in addition to phonon-phonon scattering. For a finite-length tube in which the phonons are scattered at the ends, it is more physically meaningful to use free boundary conditions in the simulations. If PBC are used, phonons will reenter the simulation box and interfere with themselves, resulting in artificial self-correlation effects at times longer than the time for the phonons to cross the simulation domain [21]. To get thermal conductivity for the micron-scale lengths used in real applications, several simulations for shorter tubes could be run to do extrapolations or parallelization could be another approach.

This paper investigates the length, temperature, and simulation method dependence of thermal conductivity for (10, 10) SWNTs. Both PBC and free boundary conditions are used. To better understand phonon modes and phonon scattering, longitudinal phonon density of states is also calculated.

COMPUTATIONAL PROCEDURE

In order to study the temperature and length dependence of thermal conductivity, four different (10, 10) SWNTs are investigated using classical MD. They have 800, 1600, 3200 and 6400 atoms, respectively. These numbers of atoms correspond to nanotube lengths of about 5, 10, 20, and 40 nm. The temperature ranges from 100K to 500K. The initial configuration of (10, 10) SWNT is constructed by using a bond length of 1.42Å. To study the effect of different boundary conditions, both free boundary and PBC are used. In PBC simulations, an extra simulation is run first with free boundaries to get the stress-free tube length. This length is very close to the original starting length.

To model the bonded carbon-carbon interactions, the second-generation reactive empirical bond order (REBO) potential is used [18]. The improved potential form can give much better description of bond energies, lengths and force constants for hydrocarbon molecules relative to the earlier Tersoff-Brenner version [17]. The interactions between non-bonded atoms are modeled using the Lennard-Jones potential.

The total bonded potential energy of the simulation system is expressed as

$$E_{pot} = \sum_i \sum_{j>i} u_B(r_{ij}) = \sum_i \sum_{j>i} [V_R(r_{ij}) - \overline{B}_{ij} V_A(r_{ij})] \quad (7)$$

The potential form in Eq. (7) appears to be pair-wise, but it should be noted that multi-body information is implicitly included in the bond order $\overline{B}_{ij}$. As in Eq. (4), the potential energy $u_B(r_{ij})$ in Eq. (7) is assumed to be split evenly between the two atoms i and j. There is more than one way to partition a many body potential among atoms, but the thermal conductivity for most cases is not sensitive to a particular partition (e.g. for silicon results computed by EMD, [22]). As the bond order potential used here does not have an explicit many body term, the partition used in Eq. (4) is reasonable. Substituting for atomic energy, the heat current expression becomes

$$\vec{J}(t) = \sum_i \vec{v}_i \varepsilon_i + \frac{1}{2} \sum_{ij, i \neq j} \vec{r}_{ij} (\vec{f}_{ij} \bullet \vec{v}_i) \quad (8)$$

The total initial linear and angular momenta are removed by subtracting the linear and angular velocity components [23]

$$\vec{v}_i^{\,new} = \vec{v}_i^{\,old} - \sum_j \vec{v}_j^{\,old} / N - \vec{\omega} \times \vec{r}_i \quad (9)$$

This procedure ensures that the isolated carbon nanotube does not have translational or rotational movement, which simplifies the calculation of the heat current along the tube axis. In all simulations, zero linear and angular momenta are well conserved. Details on the calculation of the instantaneous angular velocity of the system can be found in [24]. The resulting velocities are scaled to match the initial temperature. The time step is 1 fs for all cases. For the first 40 ps an NVT simulation with the Nosé-Hoover thermostat is used [25] to equilibrate the system to the desired temperature. Then a 400 ps long simulation is performed in the microcanonical ensemble to compute the heat current along the tube axis. The HCACF is calculated up to 200 ps, after which time it has decayed approximately to zero. A 3.4Å thickness cylinder is chosen as the geometric configuration.

In each simulation, the general expression for error propagation [26] is used to calculate the probable error of thermal conductivity

$$\sigma_k = \sqrt{\sigma_T^2 \left(\frac{\partial k}{\partial T}\right)^2 + \sigma_{<J(t)\bullet J(0)>}^2 \left(\frac{\partial k}{\partial < J(t)\bullet J(0) >}\right)^2} \quad (10)$$

Because thermal expansion of the tube is negligible [27], variation of the tube volume is not included in error estimation. The standard error of the HCACF depends on the simulation run time t_{run} and the correlation time t_{corr} [28]

$$\sigma_{<J(t)\bullet J(0)>}^2 = 2 t_{corr} < J(0)\bullet J(0) > / t_{run} \quad (11)$$

where the correlation time is defined by

$$t_{corr} = 2 \frac{\int_0^\infty (< J(t)\bullet J(0) > - < J >^2) dt}{< J^2 > - < J >^2} \quad (12)$$

RESULTS AND DISCUSSION

Temperature Dependence

For both free boundary and PBC cases, thermal conductivity decreases with increasing temperature as shown in Figure 1.

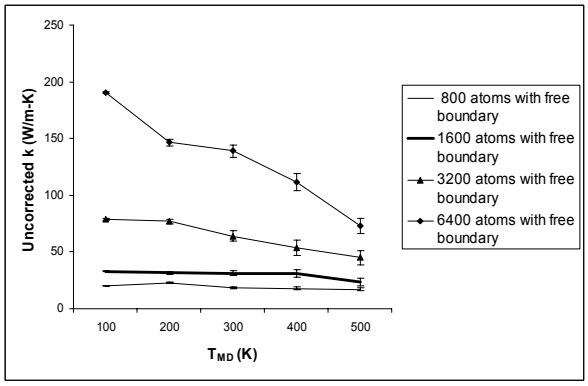

(a)

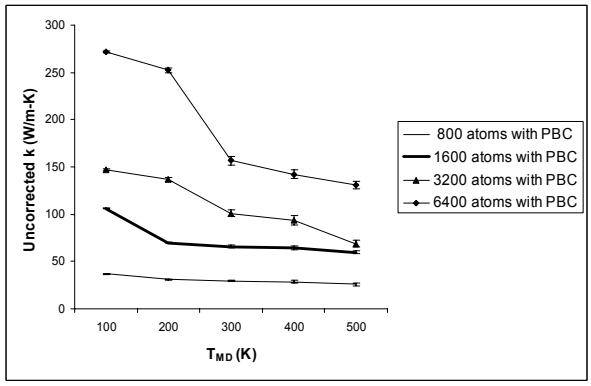

(b)

Figure 1 Thermal conductivity versus temperature for (10, 10) SWNTs of 800, 1600, 3200 and 6400 atoms with both (a) free and (b) periodic boundary conditions

Temperature in MD simulations (T_{MD}) is typically calculated from the mean kinetic energy by

$$\frac{3}{2} N k_B T_{MD} = \frac{1}{2} m \sum_{i=1}^{N} \vec{v}_i \bullet \vec{v}_i \quad (13)$$

When T_{MD} is lower than the Debye temperature, which is 2230 K for diamond and may be even higher for carbon nanotubes, quantum corrections for both temperature and thermal conductivity may be necessary especially at low temperature. By assuming the system energy to be twice the mean kinetic energy at T_{MD} and equal to the total phonon energy of the system at quantum temperature T, correction is made though [29]

$$3 N k_B T_{MD} = \int_0^{\omega_D} D(\omega) \left[\frac{1}{(e^{\hbar\omega / k_B T} - 1)}\right] \hbar \omega d\omega \quad (14)$$

where $D(\omega)$ is the phonon density of states and the zero point energy is neglected. Essentially, this procedure corrects for the low temperature specific heat variation with temperature. To get a simple estimate of the quantum correction, the 1D Debye density of states is used [30] with Debye frequency value 251

THz as the upper limit to the integral. The Debye frequency is estimated by [30]

$$\omega_D = \pi c N_{cell} / L \tag{15}$$

A 6400 atom (10, 10) SWNT has 160 unit cells and the tube length is about 40nm. The speed of sound c is taken to be 20km/s [5]. The relation between T_{MD} and T is shown in Figure 2. T_{MD} and quantum temperature T are the same at high temperatures but diverge at low temperatures.

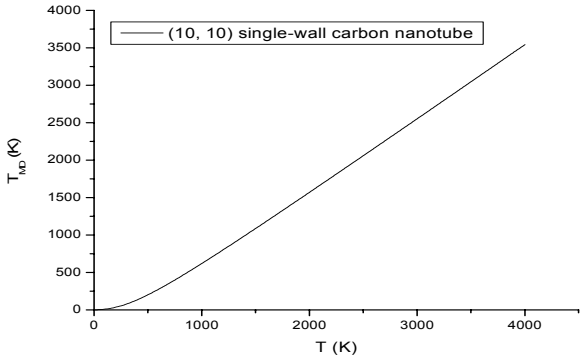

Figure 2 Relation between MD temperature T_{MD} and quantum temperature T for (10, 10) single-wall carbon nanotubes

The quantum correction is incorporated in the thermal conductivity expression by multiplying the thermal conductivity in Fourier's law by a factor dT_{MD}/dT [31]:

$$J_\alpha = -\sum_\beta k_{\alpha\beta} \partial T / \partial x_\beta = -\sum_\beta k_{\alpha\beta} (\partial T_{MD} / \partial x_\beta)(\partial T / \partial T_{MD}) \tag{16}$$

The corrected results are shown in Figure 3. They should be viewed as qualitative in nature due to the simplifying assumptions about density of states and zero point energy that have been used. The corrected thermal conductivity increases with increasing temperature and begins to decrease after 400K. This trend is consistent with thermal conductivity measurements for single-wall carbon nanotubes [2] and multi-wall carbon nanotubes [1]. It is questionable that some other studies [11-12] using classical molecular dynamics simulations can also get this peaking behavior without a quantum correction.

Effect of Boundary Condition

Figure 3 illustrates that thermal conductivity in tubes with free boundaries is lower than that with periodic boundary conditions. The reason for the jagged increase for the PBC case is not currently understood. The effect of the free boundary is to reduce the phonon lifetime due to additional scattering at the tube ends, which reduces the correlation of heat flux vector at time t with the initial heat flux vector. This reduction is very strong in the 800 atom tubes. In Figure 4 it is seen that the HCACF decays to zero very quickly and then fluctuates about this value, which leads to much lower thermal conductivity compared to that of PBC case. With increasing tube length the effect of boundary scattering is less severe, as indicated in Figure 5 for the 6400 atom free boundary case. The HCACF curve starts to have a long decaying tail and becomes similar to that of the PBC.

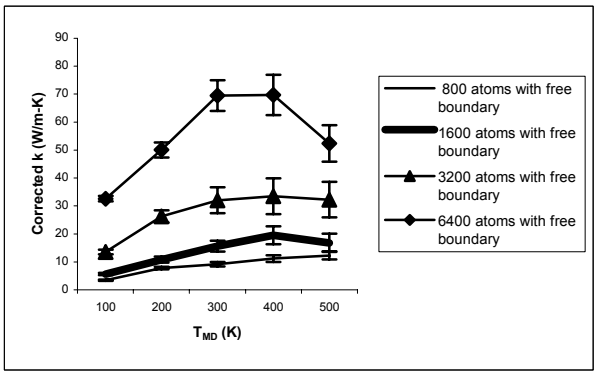

(a)

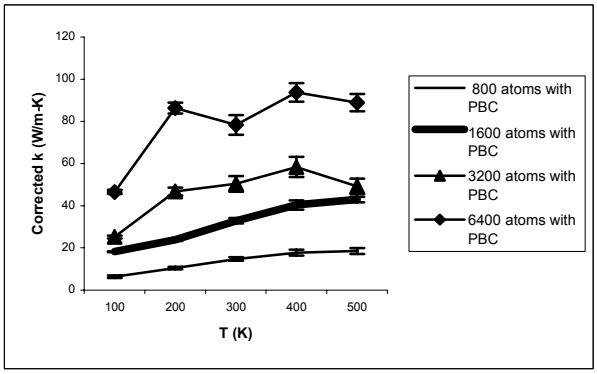

(b)

Figure 3 Quantum corrected thermal conductivity versus temperature for (10, 10) SWNTs of 800, 1600, 3200 and 6400 atoms with both (a) free and (b) periodic boundary conditions

For all PBC simulations and for free simulations of 3200 atoms or greater, the HCACF has a fast decay followed by a long lasting decay. As suggested by Che et al. [32], the decay can be fitted by a double exponential function

$$HCACF = A_1 \exp(-t/\tau_1) + A_2 \exp(-t/\tau_2) \tag{17}$$

where τ_1 and τ_2 are time constants associated with fast and slow decays, respectively. Physically τ_1 is interpreted as half of the period for energy transfer between two neighboring atoms [33]. The time constant τ_2 has been interpreted as the average phonon-phonon scattering time [33]. The double exponential fit is only performed up to a certain 'early' time which is the time a phonon takes to travel the tube. After this time self interference effects will become important and will adversely impact the HCACF. The early time is estimated in the present simulations by L/c. Thermal conductivity is found by directly integrating the HCACF before this early time after which time the fitted function is used for the integral. For all free boundary and PBC cases, τ_1 is about 10 fs showing no length or temperature dependence. In general PBC give longer decay and bigger τ_2 than free boundary conditions, which leads to higher thermal conductivity. For both cases, HCACF decays slower with increasing length, leading to a length dependent thermal conductivity.

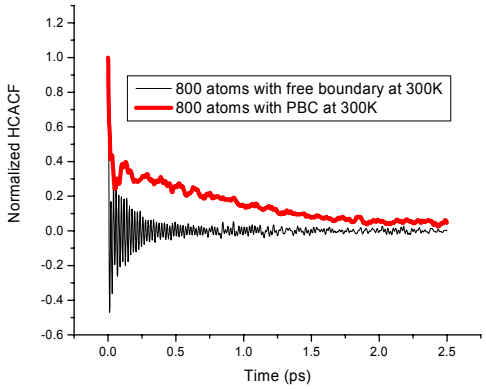

Figure 4 Normalized HCACF for (10, 10) SWNT of 800 atoms at 300K

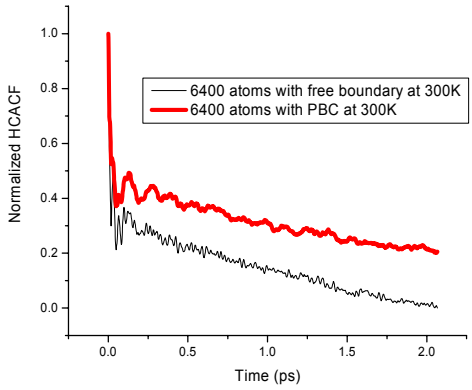

Figure 5 Normalized HCACF for (10, 10) SWNT of 6400 atoms at 300K

Length Dependence

With increased system size, more phonon modes are included and thermal conductivity is increased for both free and PBC cases shown in Figure 6. Because the longest tube length is 40nm, the thermal conductivity is still far from being converged. The thermal conductivity value is 157.92 W/m-K for 40nm tube at 300K similar to about 160W/m-K at 61.5nm long [14] and lower than the reported value 215W/m-K at 50nm long [15]. Taking the length effect into account, the reason might be that a slightly different bond order potential is used.

Figure 7 shows the time constant τ_2 versus length for PBC cases. The curves increase at low temperatures but look very flat at 400K and 500K, showing almost no length dependence. Since speed of sound tends to decrease with temperature, the double exponential function may need to be fitted to a shorter time for low temperature cases. The reason for flatness at high temperatures may be interplay between increasing number of modes that increases k and increased scattering from newly created modes which decreases k. Figures 6 and 7 have different trends: k always increasing and τ_2 flat for some cases. A simple scaling of k with τ_2, as from kinetic theory estimates of thermal conductivity, is not observed here for all cases. This may indicate that the single quantity τ_2 is not adequate to represent the detailed length-dependent thermal conductivity behavior here, which will be influenced by the addition of longer wavelength phonons that tend to have longer scattering times. Indeed, Kubo et al. [34] mentions that frequency dependent scattering is important to consider.

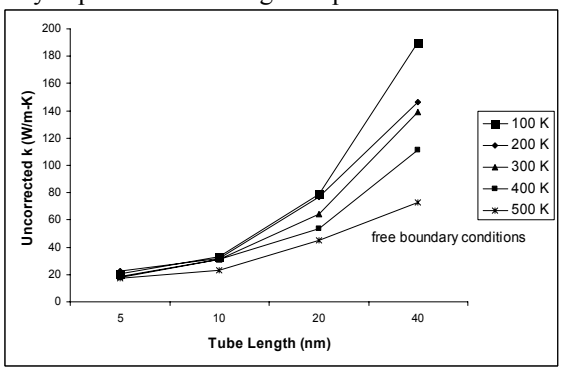

(a)

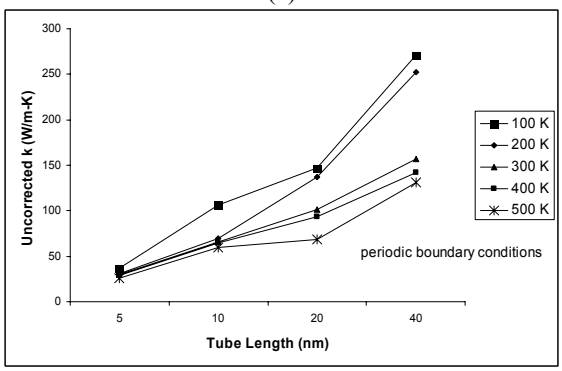

(b)

Figure 6 Thermal conductivity versus length with both (a) free and (b) periodic boundary conditions

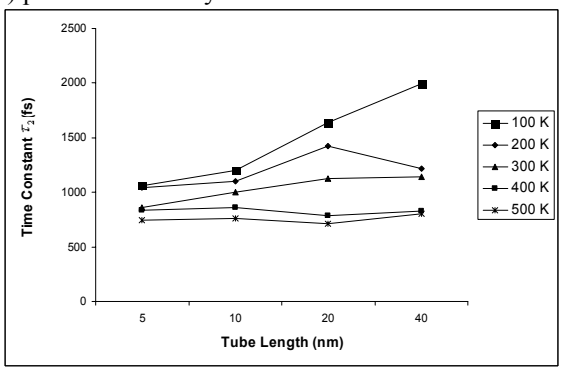

Figure 7 Time constant τ_2 versus length with periodic boundary conditions

Phonon Density of States

Thermal properties of carbon nanotubes strongly depend on the phonon density of states. Figure 8 shows the longitudinal phonon density of states at 300K for (10, 10) SWNTs with four different lengths and two different boundary conditions. This is calculated as

$$D_z(\omega) = \int dt e^{-i\omega t} < v_z(t) \bullet v_z(0) > \qquad (18)$$

4000 temporal points are used in calculating the Fourier transform of the velocity autocorrelation function. Therefore the spectral resolution is 0.25 THz. All graphs have a strong

peak around 50 THz, which is characteristic of the 2D graphene sheet phonon spectrum [35]. This value, which corresponds to a 20 fs period of vibration, agrees well with the 10 fs value of τ_1 since the characteristic time scale of energy transport at short time scales can be considered as half the period of oscillation of the carbon-carbon bond [33]. In all plots with free boundaries, there is a low frequency peak that does not exist in PBC cases. The physical meaning of this is that there is an additional vibrational mode not present in the PBC tubes. This mode represents the periodic expansion and contraction of the tube along its axis. Dickey et al. [36] also found a similar low frequency mode for small particles with free surfaces. For the 800 atom case such a peak is not easily observed, obscured by neighboring peaks. For 1600 and 6400 atoms, this peak is clearly seen. Its frequency is reduced with tube length but does not scale linearly as indicated in Table 2.

Table 2 Low frequency vibrational peaks for tubes with free boundaries

Atom number	800	1600	3200	6400
L (nm)	5	10	20	40
ν (THz)	2.25	1.25	0.75	0.5

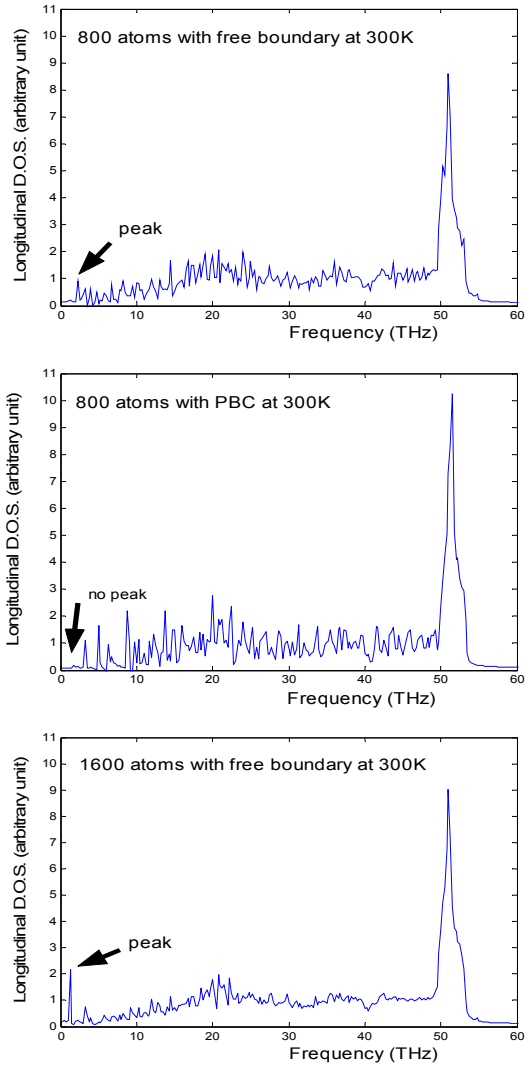

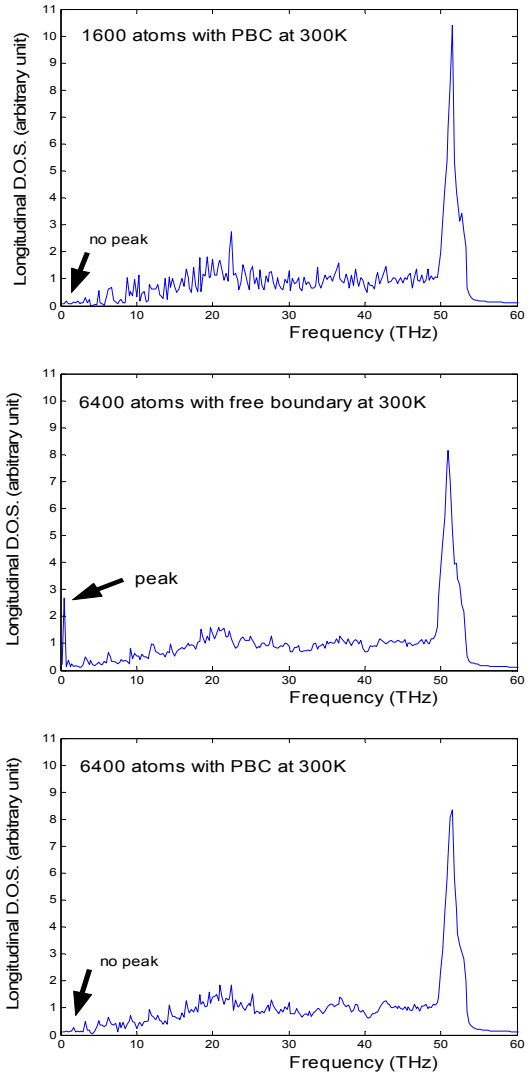

Figure 8 Longitudinal phonon density of states at 300K for (10, 10) carbon nanotubes of 800, 1600 and 6400 atoms with both free and periodic boundary conditions

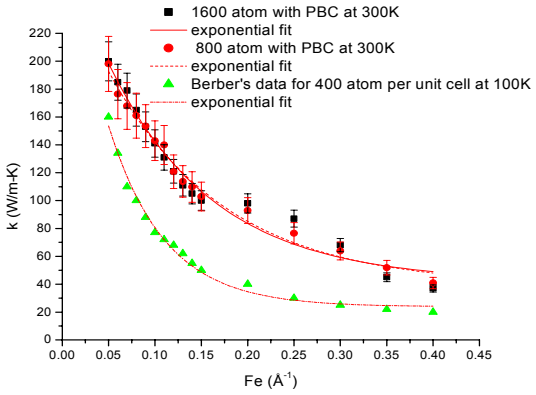

Figure 9 Thermal conductivity versus Fe

Homogeneous Nonequilibrium Molecular Dynamics

To determine the effect of MD simulation method on calculated thermal conductivity, the homogeneous NEMD method is applied to 800 atom and 1600 atom SWNTs with PBC at 300K. The thermal conductivity values and the data points at 100K taken from Berber's paper [11] are plotted in Figure 9 for comparison as their 300K data are not available.

Extrapolation to zero $\overrightarrow{F_e}$ by a single exponential fit gives thermal conductivities 267 W/m-K for 800 atom and 285 W/m-K for 1600 atom SWNT at 300K. These values are significantly higher than the corresponding values calculated in this paper by the EMD method (50 W/m-K for EMD with PBC for 1600 atom SWNT at 300K), but still much lower than Berber's reported room temperature value of 6600 W/m-K. Extrapolation of their 100K data using an exponential fit yields around 560 W/m-K at 100K, which is much smaller than their claimed 100 K extrapolation value of 37000 W/m-K.

Comparison to Literature Values

Although extrapolation using different fitting functions will result in different thermal conductivity values from homogeneous NEMD, it is not clear how the presented k versus Fe data in Berber's paper could be extrapolated to yield such a high 100 K thermal conductivity value. This also brings into question the value of 6600 W/m-K reported at 300K. Moreland et al. [15], Maruyama [16], and recently Padgett et al. [14] all used direct NEMD and found similar conductivity values, despite using different potentials and boundary conditions. Results in the present paper for both EMD and homogeneous NEMD cases are similar to those in the above three papers but are much smaller than that from Che et al. [13] who used EMD and the same boundary conditions. The only difference is the potential, REBO versus Tersoff-Brenner, which did not appear to play a significant role in the three direct NEMD simulations above. The reason for the difference between Che's and the present data are thus still not clear, although scaling by the same cross sectional area reduces the discrepancy to a factor of 3-4. Osman et al. [12] used the same NEMD and heat flux control technique as Padgett et al. [14] but got much higher values. At present, these discrepancies are also not understood, unless they are a result of stress or some other unknown factor. As the majority of reported values, including the values in the present paper, are of the order of a few hundred W/m-K for the tube lengths considered, and because the papers in agreement are more recent than those reporting very high thermal conductivities, it is believed that the simulations reporting lower thermal conductivity are more likely to be correct. The ultimate test of correctness is, however, similarity to experimental data. The 'correct' simulations in Table 1 are an order of magnitude lower than available experimental data, but are also performed on tubes that are short (< 100 nm) relative to the expected experimental lengths of a few microns in order to enable comparison of a variety of papers. Simulations on longer tubes (400 nm [16] and 1000 nm [15]) indicate that thermal conductivity has still not converged and will continue to increase with tube length. This behavior is expected due to the long phonon mean free path and is a likely reason for the low 'correct' values. Additionally, the homogeneous NEMD method yields values almost a factor of 6 higher for the EMD method for the same tube length. This indicates that calculated values approaching experimental values may be attainable for simulations performed on sufficiently long tubes. It remains to be seen whether differences in intermolecular potential will have a significant effect at longer tube lengths.

CONCLUSIONS

Using molecular dynamics simulations we have calculated the thermal conductivity for (10, 10) single-wall carbon nanotubes as function of temperature, length, and simulation method for both free boundary and periodic boundary conditions. To qualitatively account for the quantum effect, a correction is made to the thermal conductivity. The corrected values increase with increasing temperature and fall off at high temperature showing a trend that is consistent with experimental observations. The free boundaries reduce phonon lifetime due to additional phonon scattering at tube ends and therefore give lower thermal conductivity than that of periodic boundary conditions. Thermal conductivity increases with length at all temperature and boundary conditions but still shows no convergence at the longest tube length 40nm. An uncorrected value of about 160 W/m-K is found at 300K for this tube length using equilibrium molecular dynamics. Homogeneous nonequilibrium molecular dynamics simulation indicates a factor of ~6 increase as compared to equilibrium molecular dynamics for 10 nm tubes at 300K (285 vs. 50 W/m-K). The time constant τ_2 of the double exponential fit for the heat current autocorrelation function increases with length at low temperature but shows no length dependence at high temperatures. It remains to be seen how appropriate a single frequency independent value is in predicting thermal conductivity. Comparison of the present values to those reported previously indicate that the lower values calculated in Refs. [14-16] are more likely to be correct than the others. Discrepancies between simulated and experimental values are attributed to length effects, and may also arise the effects of simulation method, stress, and intermolecular potential.

ACKNOWLEDGMENTS

This work is supported by the Office of Naval Research (grant no. N00014-03-1-0890).

REFERENCES

1. Kim, P., Shi, L., Majumdar, A. and McEuen, P. L., Mesoscopic Thermal Transport and Energy Dissipation in Carbon Nanotubes, Physica B 323, pp. 67-70, 2002.
2. Hone, J., Whitney, M., Piskoti, C. and Zettl, A., Thermal Conductivity of Single-walled Nanotubes, Physical Review B, Vol. 59, no. 4, pp. 2514-2516, 1999.
3. Yu, C., Jang, W., Hanrath, T., Kim, D., Yao, Z., Korgel, B., Shi, L., Wang, Z. L., Li, D. and Majumdar, A., Thermal and Thermoelectric Measurements of Low Dimensional Nanostructures, *Proc. 2003 ASME Summer Heat Transfer Conference*, HT2003-47263, pp.1-6, 2003.
4. Haile, J. M., *Molecular Dynamics Simulation: Elementary Methods*, John Wiley & Sons, Inc., New York, 1992.

5. Dresselhaus, M. S. and Eklund, P. C., Phonons in Carbon Nanotubes, Advances in Physics, Vol. 49, no. 6, pp. 705-814, 2000.
6. Hoover, W. G. and Ashurst, W. T., Nonequilibrium Molecular Dynamics, Theoretical Chemistry: Advances and Perspectives, Vol. 1, H. Eyring and D. Henderson, eds., Academic Press, New York, pp. 1-51, 1975.
7. Frenkel, D. and Smit, B., *Understanding Molecular Simulation: From Algorithms to Applications*, Academic Press, 2001.
8. Hansen, J. P. and McDonald, I. R., *Theory of Simple Liquids*, Academic Press, London, 2nd edition, 1986.
9. Irving, J. H. and Kirkwood, J. G., the Statistical Mechanical Theory of Transport Processes. IV. The Equations of Hydrodynamics, Journal of Chemical Physics, Vol. 18, pp. 817-829, 1950.
10. Evans, D. J., Homogeneous NEMD Algorithm for Thermal Conductivity – Application of Non-Canonical Linear Response Theory, Physics Letters, Vol. 91A, No. 9, pp. 457-460, 1982.
11. Berber, S., Kwon, Y. and Tomanek, D., Unusually High Thermal Conductivity of Carbon Nanotubes, Physical Review Letters, Vol. 84, no. 20, pp. 4613-4616, 2000.
12. Osman, M. A. and Srivastava, D., Temperature Dependence of the Thermal Conductivity of Single-wall Carbon Nanotubes, Nanotechnology 12, pp. 21-24, 2001.
13. Che, J., Çağin, T., Deng, W. and Goddard III, W. A., Thermal Conductivity of Carbon Nanotubes, Nanotechnology 11, pp. 65-69, 2000.
14. Padgett, C. W. and Brenner, D. W., Influence of Chemisorption on the Thermal Conductivity of Single-Wall Carbon Nanotubes, Nano Letters, Vol. 4, No. 6, pp. 1051-1053, 2004.
15. Moreland, J. F., Freund, J. B. and Chen, G., The Disparate Thermal Conductivity of Carbon Nanotubes and Diamond Nanowires Studied by Atomistic Simulation, Microscale Thermophysical Engineering 8, pp. 61-69, 2004.
16. Maruyama, S., Molecular Dynamics Simulation of Heat Conduction of a Finite Length Single-walled Carbon Nanotube, Microscale Thermophysical Engineering 7, pp. 41-50, 2003.
17. Brenner, D., Empirical Potential for Hydrocarbons for Use in Simulating the Chemical Vapor Deposition of Diamond Films, Phys. Rev. B, Vol. 42, no. 15, pp. 9458-9471, 1990.
18. Brenner, D. W., Shenderova, O. A., Harrison, J. A., Stuart, S. J., Ni, B. and Sinnott, S. B., A Second-generation Reactive Empirical Bond Order (REBO) Potential Energy Expression for Hydrocarbons, J. Phys.: Condens. Matter 14, pp. 783-802, 2002.
19. Abramson, A.R., Tien, C.L. and Majumdar A, Interface and Strain Effects on the Thermal Conductivity of Heterostructures: A Molecular Dynamics Study, Journal of Heat Transfer, 124(5): pp. 963-970, 2002.
20. Shi, L., *Mesoscopic Thermophysical Measurements of Microstructures and Carbon Nanotubes*, Ph.D. thesis, University of California, Berkeley, 2001.
21. Volz, S. G., and Chen, G., Molecular-dynamics Simulation of Thermal Conductivity of Silicon Crystals, Physical Review B, Vol. 61, No. 4, 2000.
22. Schelling, P. K., Phillpot, S. R. and Keblinski, P., Comparison of Atomic-level Simulation Methods for Computing Thermal Conductivity, Physical Review B, Vol. 65, pp. 144306-144317, 2002.
23. Zhou, Y., Cook, M. and Karplus, M., Protein Motions at Zero-Total Angular Momentum: The Importance of Long-Range Correlations, Biophysical Journal, Vol. 79, pp. 2902-2908, 2000.
24. Goldstein, H., *Classical Mechanics*, Reading, MA, Addison-Wesley, 1980.
25. Hoover, W. G., Canonical dynamics: Equilibrium phase-space distributions, Physical review A, Vol. 31, no. 3, pp. 1695-1697, 1985.
26. Press, W. H., Teukolsky, S. A., Vetterling, W. T. and Flannery, B. P., *Numerical Recipes in FORTRAN: The Art of Scientific Computing*, 2nd Ed., Cambridge University Press, Cambridge, UK, 1992.
27. Schelling, P. K. and Keblinski, P., Thermal Expansion of Carbon Structures, Physical Review B 68, 035425, 2003.
28. Allen, M. P. and Tildesley, D. J., *Computer Simulation of Liquids*, Clarendon Press, Oxford, UK, 1987.
29. Maiti, A., Mahan, G. D. and Pantelides, S. T., Dynamical Simulations of Nonequilibrium Processes – Heat Flow and Kapitza Resistance Across Grain Boundaries, Solid State Communications, Vol. 102, pp. 517-521, 1997.
30. Ashcroft, N. W. and Mermin, N. D., *Solid State Physics*, Harcourt College Pub, 1976.
31. Lee, Y. H., Biswas, R., Soukoulis, C. M., Wang, C. Z., Chan, C. T. and Ho, K. M., Molecular-dynamics Simulation of Thermal Conductivity in Amorphous Silicon, Physical Review B, Vol. 43, no. 8, pp. 6573-6580, 1991.
32. Che, J., Çağin, T., Deng, W. and Goddard III, W. A., Thermal Conductivity of Diamond and Related Materials from Molecular Dynamics Simulations, Journal of Chemical Physics, Vol. 113, No. 16, pp. 6888-6900, 2000.
33. McGaughey, A. J. H. and Kaviany, M., Thermal Conductivity Decomposition and Analysis Using Molecular Dynamics Simulations. Part I. Lennard-Jones Argon, International Journal of Heat and Mass Transfer 47, pp. 1783-1798, 2004.
34. Kubo, R., Toda, M. and Hashitsume, N., *Statistical Physics II*, Springer, Berling, 1985.
35. Sokhan, V. P., Nicholson, D. and Quirke, N., Phonon Spectra in Model Carbon Nanotubes, Journal of Chemical Physics, Vol. 113, no. 5, pp. 2007-2015, 2000.
36. Dickey, J. M. and Paskin, A., Size and Surface Effects on the Phonon Properties of Small Particles, Physical Review B, Vol. 1, No. 2, pp. 851-857, 1970.